

# Modification of Gel-Drawn Poly(vinyl Alcohol) Fibers with Formaldehyde

DAVID T. GRUBB and F. RICH KEARNEY, *Department of Materials Science and Engineering, Cornell University, Ithaca, New York 14853*

## Synopsis

Poly(vinyl alcohol) fibers which were drawn from dried gels were chemically treated with formaldehyde to induce crosslinking in the amorphous phase. The room temperature storage modulus decreased early in the treatment, to an almost constant value of 50–60% of the initial modulus of the fiber. This behavior was independent of the concentration of formaldehyde used. The modulus at low temperature was also reduced, and no  $T_g$  peak could be seen in heavily treated fibers. The modulus above the original  $T_g$ , 70°C, was much less affected. The crystallinity determined by DSC fell by one third as the room temperature modulus decreased, and X-ray diffraction indicated a reduction in the crystal length along the chain direction at the same time. Thus, under the conditions of treatment used, the loss of properties due to destruction of crystals outweighs the stiffening and reduced water sensitivity of the crosslinked amorphous phase.

## INTRODUCTION

Poly(vinyl alcohol) (PVAL) is normally atactic and has a high concentration of head-to-head defects, but it is nevertheless semicrystalline. It is prepared by saponification of an ester, and if this reaction is incomplete, an amorphous and water-soluble copolymer is produced, which is still called poly(vinyl alcohol). Both wet-spinning and dry-spinning methods have been used commercially to produce fibers of semicrystalline PVAL with tensile moduli of 7.8–28 GPa.<sup>1</sup> Since the chain structure of crystalline PVAL is all-trans, like that of polyethylene, its crystal modulus in the chain direction is predicted to be in the range of 300–400 GPa. Thus fibers of even higher performance might be prepared from PVAL.<sup>1–5</sup>

Drawing of dried gels to high draw ratios has been proposed as a method of producing such high-modulus PVAL fibers, and several papers have been published on drawn PVAL gel fibers.<sup>3,6–9</sup> The most successful methods of gel drawing are those involving a short residence time within a heated drawing zone. Kwon et al.<sup>2</sup> have produced PVAL fibers from glycerin and ethylene glycol gels with tensile moduli of up to 75 GPa and tensile strengths ranging from 0.4 to 2.6 GPa. Another method<sup>8,7</sup> produces draw ratios of 15–40 and moduli of 15–35 GPa by the use of a small contact heater.

Although these values are sufficiently high to make these fibers useful for some commercial applications, PVAL shows a strong tendency to absorb water, which acts as a plasticizer. Tensile moduli for PVAL fibers decrease measurably with water absorption, and  $T_g$  decreases as a function of water content.<sup>1,8</sup> Fiber tenacity for wet-spun fibers also falls by 17% on absorption of water.<sup>1</sup>

Sakurada and Nakamura<sup>10</sup> have shown that treatment of PVAL with formaldehyde under acidic conditions decreases the amount of water absorption. Formaldehyde forms an acetal with polyalcohols under acidic conditions, which lowers their affinity toward water. If the formalization is performed by diffusing the reactants into the solid, further water resistance is achieved by the formation of acetal crosslinks.<sup>11</sup> The morphology of the solid also influences the final swelling state, as the crystalline regions of PVAL are impermeable to water at temperatures below 80°C, so that crosslinking only occurs in amorphous regions.<sup>12,13</sup> This method of improving water resistance has been applied to wet-spun PVAL fibers<sup>1</sup> with reasonably good success.

In this study PVAL tapes were produced by zone drawing strips of dried gel over a small contact heater as described by Garrett and Grubb.<sup>8</sup> Although the samples were geometrically narrow tapes, wide angle X-ray diffraction with the beam parallel to the fiber axis showed that their structure had fiber symmetry, and we will describe them as fibers. The fibers were treated with formaldehyde under conditions similar to those used in the commercial formalization of wet-spun PVAL. The mechanical and structural properties of the formalized fibers were investigated to determine the effects of this chemical modification. In particular, the storage modulus and loss tangent were obtained from -70 to 150°C, and the crystallinity, crystal size, and SAXS long period were determined.

## EXPERIMENTAL

PVAL was obtained from Polysciences; it was found to be atactic and 100% saponified and had a weight-average MW of 151,000 and a polydispersity of 1.7. Gels were prepared from a 2:1 mixture of ethylene glycol and water, were dried, cut into strips, and zone drawn at 2 in./min by the method of Garrett and Grubb.<sup>7,8,9</sup> Gels were drawn to an average draw ratio of either 13-15 or 20-25. A typical sample cross section was  $\sim 1 \times 0.1$  mm, and fiber length varied from 6 to 9 cm, depending on draw ratio.

The storage modulus  $E'$  at 110 Hz and room temperature (20°C) was measured for all the untreated fibers in the dry state with a Rheovibron DDV-II. All tests were performed while passing nitrogen dried over  $P_2O_5$  through the sample chamber. It was found that the fibers drawn to 13-15 times had a storage modulus in the range 13-14 GPa. The fibers drawn to 20-25 times had a wider range of stiffness, from 19 to 27 GPa. Two groups were selected from these stiffer fibers for further testing, one with moduli of 20-21 GPa and one with 25-26 GPa. For the remainder of this paper, groups of treated fibers will be referred to by their initial storage modulus  $E_0$  as 13, 21, or 25 GPa.

Fibers were treated with formaldehyde using an aqueous solution containing 15 wt % sulfuric acid, 10 wt % sodium sulfate, and either 1, 3, or 5 wt % formaldehyde. The formaldehyde was added in the usual commercial form of a 35% solution in water. Treatment times were 10-90 min at 72°C; the treated fibers were then washed in distilled water for 1 h, dried overnight in air, and stored over  $P_2O_5$  for at least 24 h. The temperature of treatment was chosen to be similar to that of commercial PVAL fiber formalization, and to give a uniformly treated fiber.

Since the thickness of the tapes used was 0.1 mm, the crosslinking might well have limited diffusion of the reactant to the center of the sample. This was found not to be the case. Formaldehyde treated samples from the 21 GPa set were treated with 0.02M ammonium dichromate solutions in the dark for 48 h at room temperature, followed by a 1-h exposure to a 150-W "black light" UV light source ( $\lambda = 350$  nm). The sample darkens by reaction of the hydroxyl groups of PVAI and  $\text{Cr}_2\text{O}_4^{2-}$  to form  $\text{Cr}_2\text{O}_3$  and ketone groups on the main chain. Chromium stained samples were mounted in epoxy and polished to flatness with the cross section of the fiber exposed. The chromium profile was then determined in an electron microprobe by scanning the main beam across the sample while detecting the characteristic emitted X-rays at the  $\text{CrK}_\alpha$  line. The stain was homogeneous throughout the fiber, indicating a uniform degree of formalization.

Three groups 21 GPa fibers were treated with formaldehyde as described above, one each at 1, 3, and 5% formaldehyde concentration. One group of 13 GPa fibers and one group of 25 GPa fibers were also treated with 3% formaldehyde. The storage modulus  $E'$  at 110 Hz and room temperature was again measured for all the treated fibers in the dry state. All fibers treated with 3% formaldehyde solution were also tested by dynamic mechanical analysis of over a temperature range of  $-70$  to  $150^\circ\text{C}$  at a heating rate of  $3^\circ\text{C}/\text{min}$  to determine  $T_g$ .

Differential scanning calorimetry was performed for each sample on a Perkin-Elmer DSC-2C interfaced to an IBM PC-XT. Samples were prepared by cutting a 3–4 mm piece from the end of a fiber and placing the piece in a sample pan with a small amount of oil to allow shrinkage during melting. The test was done with no lid on the pan. The degree of crystallinity  $\chi_c$  was determined from the area of the melting peak using  $156.2$  J/g as the enthalpy of fusion for PVAI crystals.<sup>14</sup> In addition, the length of each DSC sample was measured using an Olympus microscope before and after thermal analysis, to measure shrinkage. Molecular extension was determined from fiber shrinkage as (original length/final length).<sup>15</sup>

Wide angle X-ray scattering patterns were obtained using a  $\text{CuK}_\alpha$  source at 35 kV and 14 mA, and a Statton camera with flat-plate geometry. The camera length was 5 cm and a single fiber was mounted perpendicular to the beam. An exposure time of 48 h was required. In the monoclinic crystal structure of PVAI, the chain direction is perpendicular to the  $(0k0)$  planes. The  $(010)$  reflection is forbidden, and it is the  $(110)$  reflection which appears on the meridian at the first-order layer line when the fiber is perpendicular to the beam. This is because the  $(110)$  normal is  $17^\circ$  to the fiber axis, and this is also its Bragg angle for  $\text{CuK}_\alpha$  X-rays. The intensity profiles for the  $(110)$  and  $(002)$  reflections were deconvoluted with the instrumental broadening function as determined by scattering from  $0.5$   $\mu\text{m}$  grain alumina powder. Crystal size in the direction perpendicular to these planes was measured from the integral breadth of the reflection after this deconvolution. A lower limit was determined by using the Scherrer formula and assuming no contribution from crystal imperfection.

The  $(020)$  peak width was measured with a Braun position sensitive detector using  $\text{CuK}_\alpha$  radiation. Samples were prepared by gluing small sections of fiber together at their ends to form a stack about 0.75 mm thick. The sample

was tilted at the Bragg angle,  $37^\circ$  for (020), from the perpendicular to incident beam. The detector was mounted at twice this angle,  $74^\circ$  from the perpendicular to the beam direction, to avoid broadening due to the finite depth of the sensitive region of the detector. The sample to detector distance was 58 mm and data collection time was 600 s. The instrumental broadening due to beam size and divergence was determined from the width of the (220) peak from a thin copper foil. It was assumed that this broadening and the crystal size effect would both give a Gaussian profile, and that the fiber sample thickness adds a "top hat" profile to this. The "top hat" width was calculated from the specimen thickness and the diffraction geometry and the effect on the full width at half maximum (fwhm) of convoluting Gaussian and "top hat" profiles was numerically modelled. This allowed measurement of the crystal size in the (020) direction, again assuming no contribution from crystal imperfection.

The small angle X-ray scattering (SAXS) peaks produced by the PVAI fibers were weak, so that SAXS was performed at the Synchrotron radiation source CHESS. The double focussed monochromatic beam at station A1 was used, with a point collimator 0.3 mm in diameter. Data were collected using a Reticon linear diode array collector of 25- $\mu\text{m}$  spatial resolution at a camera length of 60 cm and an OMA II multichannel analyzer. All the fibers showed a well-defined small angle peak. The intensity was Lorentz-corrected by a factor of  $s^2$  before determining the peak position, but the correction made little difference.

## RESULTS AND DISCUSSION

Figure 1 shows the storage modulus of the PVAI fibers at  $20^\circ\text{C}$  and 110 Hz as a function of treatment time in formaldehyde solution. The three lines in Figure 1 show the moduli of the three groups of fibers treated with 3% formaldehyde solution. The error bars are the calculated errors in the modulus, which are largely due to uncertainty in the measurement of fiber cross section. Although there is some irregularity,  $E'$  drops rapidly in the first 20–30 min of treatment, after which it remains approximately constant. The lines maintain their order, so that the final (90-min) modulus depends on the initial fiber modulus, being 50–60% of  $E_0$ . The remaining data points shown in Figure 1 are for fibers with  $E_0 = 21$  GPa treated with 1 or 5% formaldehyde solution. This data is somewhat more scattered, but follows the same trend as the lines in Figure 1. The data for treatment in the 5% solution are sometimes above and sometimes below the data for treatment in 3 or 1% solution. There is no indication that the rate of modulus loss or the modulus level at long treatment times is affected by the concentration of formaldehyde in the treatment bath.

Figure 2 shows the results of dynamic mechanical analysis of fibers with  $E_0 = 21$  GPa treated with 3% formaldehyde solutions for 0–90 min, as indicated. The temperature dependence of  $\tan \delta$ , the lower plots in Figure 2, show that the untreated fiber has a characteristic  $T_g$  peak at about  $70^\circ\text{C}$  and low values of  $\tan \delta$  below  $40^\circ\text{C}$ . There is a slight indication of a broad peak at  $-10^\circ\text{C}$ . After 10 min formalization a  $T_g$  peak is still seen, but it is shifted to a lower temperature and superposed on a broad background. After 20 min

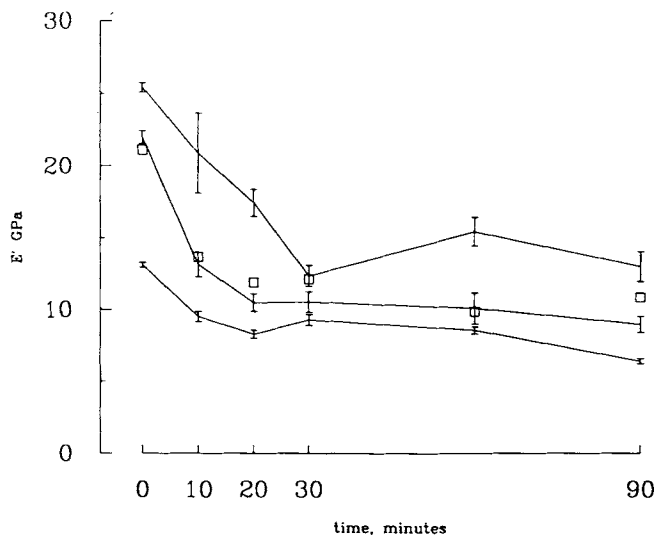


Fig. 1. Storage modulus of poly(vinyl alcohol) (PVAL) fibers measured at 110 Hz and 20°C as a function of time of treatment in 3% formaldehyde solution. The lines are drawn through data sets for initial modulus of 25, 21, and 13 GPa. The remaining data points are for fibers of initial modulus of 21 GPa treated with formaldehyde solutions of 1% (\*) and 5% (□) concentration.

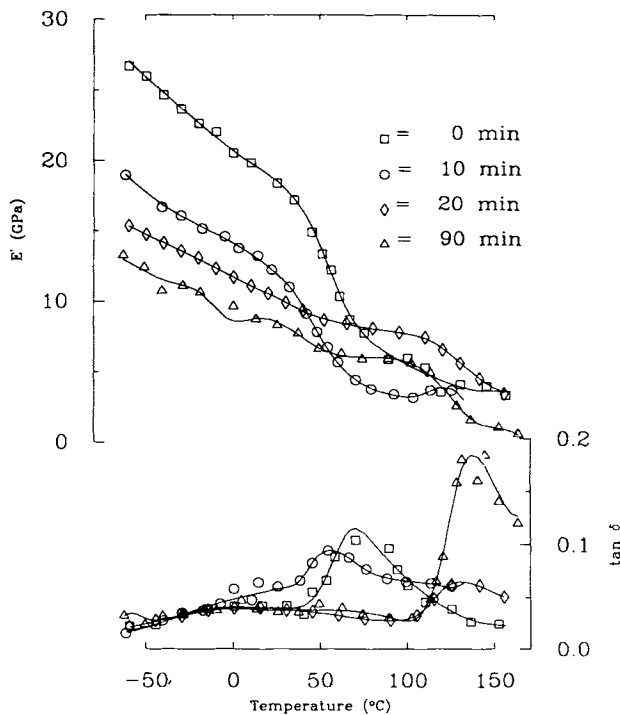


Fig. 2. Temperature dependence of the storage modulus and loss tangent for PVAL fibers of initial modulus 21 GPa at increasing treatment times in 3% formaldehyde solution.

treatment, the background has returned to its initial low value below 40°C and no  $T_g$  peak can be observed. In addition, a peak appears at  $T \approx 130^\circ\text{C}$  after 20 min. Further treatment increases the intensity of the high temperature peak, but there is no change below 100°C. When the high-temperature peak appears, the fiber begins to blacken during the test. It seems that the high temperature loss peak is associated with chemical degradation and not a physical relaxation.

The storage modulus data presented in the upper plot of Figure 2 show that the modulus at low temperatures is reduced by formaldehyde treatment to a greater degree than at room temperature, partly because 20°C is actually within the inflection of the curve caused by  $T_g$ . When the glass transition has been suppressed, at 20 and 90 min treatment according to the  $\tan \delta$  curves, there is no longer such an inflection in the modulus vs. temperature curve. At 70°C and above the modulus of these treated fibers is close to or greater than the modulus of the untreated fiber, and the variation with temperature is small until the onset of degradation at  $T \geq 105^\circ\text{C}$ . Data for  $E_0 = 25$  and 13 GPa showed similar results.

In dilute solution, formalization of PVAI produces a random copolymer of poly(vinyl alcohol) and poly(vinyl formal). The  $T_g$  of the copolymer should be somewhere between that of the parent PVAI, which is 80°C<sup>1</sup> or 70°C by our measurement, and that of poly(vinyl formal) which is 108°C.<sup>16</sup> The actual value of  $T_g$  of copolymers is normally explained by one of a number of empirical mixing laws, but, in any case,  $T_g$  should rise slightly on formaldehyde treatment. Here the reaction is occurring in the swollen solid, so that crosslinking is also expected to occur. Crosslinking increases the constraints on chains, so that generally increases  $T_g$ . It makes the material less homogeneous and so broadens the relaxation. As constraints increase further with increasing crosslink density, no  $T_g$  peak can be observed and the sample is glassy at all temperatures.

The  $T_g$  peak does broaden and eventually disappear on treatment with formaldehyde, but the predicted rise in peak temperature is not observed. A possible explanation for this is that the constraints on the amorphous chains are being affected by changes in the crystalline phase.  $T_g$  in crystallizable polymers can increase with crystallinity  $\chi_c$ ,<sup>17</sup> as the crystals limit the motion of amorphous chains. A decrease in  $\chi_c$  could thus cause some reduction in  $T_g$ ; it would also explain the reduction in modulus at low temperatures, where unmodified and modified amorphous material should have much the same modulus.

The melting of highly drawn fibers often produces irregular endotherms, such as in Figure 3. This is caused by parts of the sample being under different constraints, sticking to the sample pan or shrinking erratically, and makes melting point difficult to determine. The melting peaks shown in Figure 3 are from treated samples and these were more irregular than those obtained from untreated fibers. Although the melting points could not be determined, treatment with formaldehyde always reduced the temperature of the onset of melting. Irregularity of the melting peak should not affect the enthalpy of fusion, determined from the area of the curve. In these samples measurement of enthalpy of fusion was hampered by the presence of a large broad endotherm just above the melting point, as shown in Figure 3(a). This peak

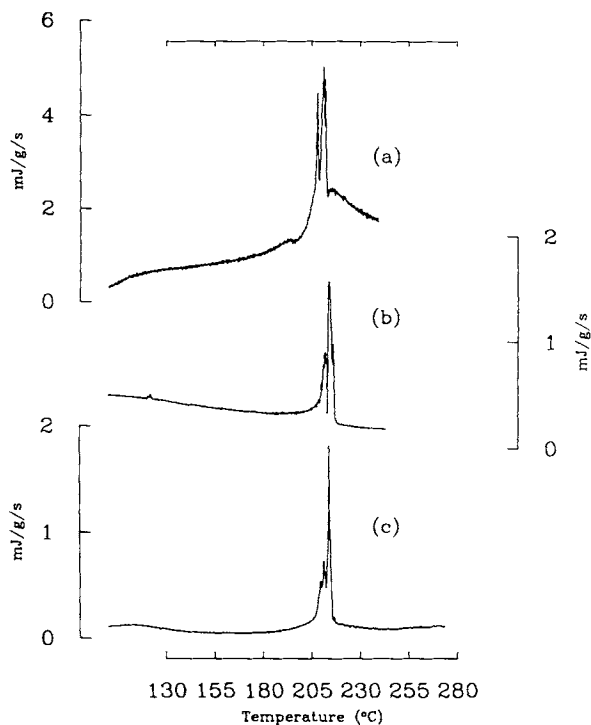


Fig. 3. DSC melting scans for a PVAI fiber of initial modulus at 25 GPa, 60-min reaction time in 3% formaldehyde solution: (a) initial dry fiber; (b) 2% water content, after exposure to room moisture; (c) redried fiber.

appeared in all samples which had been dried over  $P_2O_5$  for several days to assure accurate mass measurement. When the same fibers were allowed to absorb water in air overnight, the broad peak disappeared [Fig. 3(b)].

While in most cases the value of  $\chi_c$  was obtained from subtracting a background from peaks such as that in Figure 3(a), the value was equal to that obtained by integrating the melting endotherm of peaks as in Figure 3(b) and correcting the mass for swelling by water. If  $\chi_c$  was determined from 3(a) including the broad endotherm, crystallinity values over 100% were obtained, which is not possible. When a fiber was allowed to absorb water and was then redried, the broad endotherm returned. It was not as large as before [Fig. 3(c)] perhaps because drying was not so complete. PVAI undergoes thermal degradation near the melting point<sup>14,18</sup> by dehydration of the main chain. A similar reaction involving formal groups could be the source of the broad endotherm, if this reaction is affected by water in the sample.

The crystallinity as determined by heat of fusion decreased with formaldehyde treatment, as shown in Figure 4. The average and rms deviation for all starting conditions is plotted since  $\chi_c$  had a large amount of scatter with no systematic dependence on initial modulus or formaldehyde concentration. Within 10 min,  $\chi_c$  has fallen from 62 to 45%, and then the fall is much slower. The line drawn in Figure 4 is the fit to data for all treated fibers, and falls 1% in crystallinity in each 12 min. But it is apparent from the scatter in the data that a limiting value of  $40 \pm 2\%$  for all initial conditions is as good a

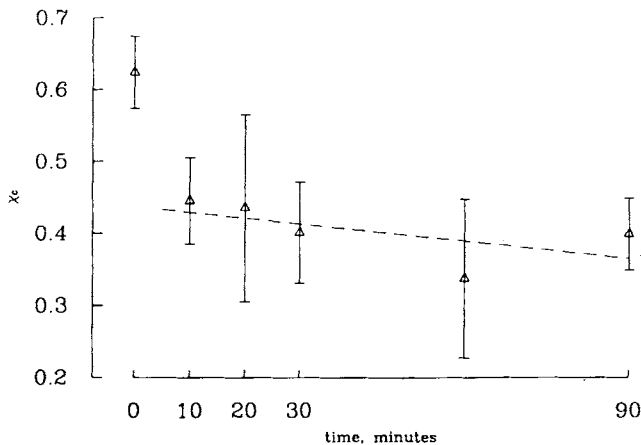


Fig. 4. Crystallinity of PVAL fibers as a function of treatment time in all formaldehyde concentrations studied.

description for the crystallinity of formaldehyde-treated fibers. The crystallinity of all the fibers fell by 30% in the first 10 min of treatment, so that the modification of fiber morphology is rapid.

The shrinkage of the PVAL fibers followed the same pattern of behavior as the crystallinity. Individual results showed no dependence on starting condition. The initial value of shrinkage was  $8 \pm 0.7$  and by 20 min of treatment this fell to a constant value of  $4 \pm 0.5$ . Radiation crosslinking studies in polyethylene fibers<sup>19</sup> have shown that fiber shrinkage decreases with increasing crosslink density, so that the reduction of shrinkage upon melting implies the introduction of effective crosslinks. This would also indicate that the crosslink density approaches a maximum after 20 min, presumably when the material either cannot accept more formal groups due to the exhaustion of adjacent hydroxyls by irreversible reaction, or when the material cannot swell further to receive more cross-linking reagent. It is likely that both factors are important.

A lower limit for the mean crystal size perpendicular to the fiber direction was determined from the integral breadth of the (200) direction. The crystal size in the (200) direction was taken to be representative of all dimensions perpendicular to the fiber axis, which is equivalent to assuming circular cross section for the fibrous crystals. The integral breadth of the (110) reflection, which is  $18^\circ$  from the fiber axis, was used in a similar way to determine the crystal size in a direction close to the fiber axis. If the crystals are much longer than they are wide, this can give misleading results, so that later the width of the (020) reflection was measured to give a more direct estimate of the axial size of the fibrous crystals, for fibers with  $E_0$  21 GPa treated in 3% formaldehyde. Figure 5 summarizes the WAXS data described above. Both measures of axial crystal size, the (110) and (020) reflections, show a sharp decrease at 10 min, a slight recovery at 20 min, and then a constant value. For (110) the values are 85 to 68 to 72 Å; for (020) they are 114 to 95 to 100 Å. In contrast, the width of the fibrous crystals in the direction perpendicular to the fiber



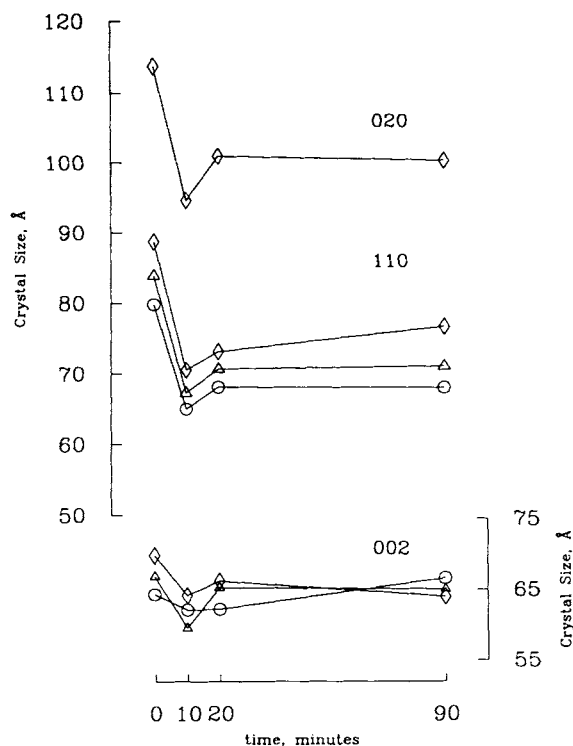


Fig. 5. Dependence of crystal size in the indicated crystallographic directions on treatment time in 3% formaldehyde solution: (○)  $E_0 = 25$  GPa; (◇)  $E_0 = 21$  GPa; (△)  $E_0 = 13$  GPa. Note that (020) is the direction of the chain axis.

axis decreases very slightly if at all, from 67 to 65 Å. This final value is independent of initial modulus.

The SAXS long period is plotted in Figure 6. Although the 21 GPa fibers showed large variations at short treatment times, which cannot be explained, the overall trend is that the long period remains constant or decreases only slightly. For all treatment times and draw ratios, Figure 6 indicates a fall of

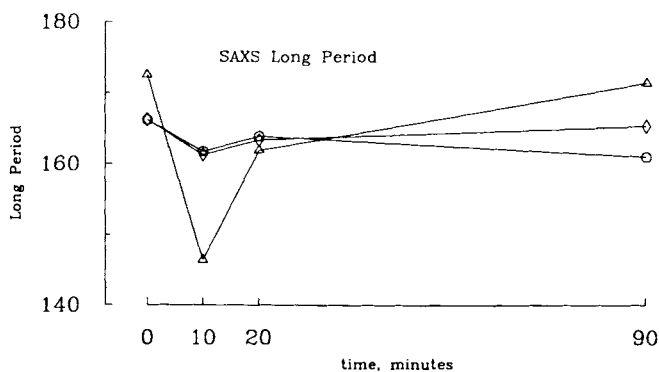


Fig. 6. Variation of SAXS Long period with treatment time in 3% formaldehyde solution: (○)  $E_0 = 25$  GPa; (◇)  $E_0 = 21$  GPa; (△)  $E_0 = 13$  GPa. Data symbols correspond to those of Figure 5.

only 6 Å, from 168 to 162 Å. This is constant within experimental error, so that the long period is unchanged by the chemical treatment. The ratio of (020) crystal size to SAXS long period drops from 0.68 to 0.61 on formaldehyde treatment. This small drop in "linear crystallinity" may indicate that many crystals are being totally destroyed. Since the SAXS peak intensity is low, another possible explanation is that the periodic structure which gives rise to it may not be representative of all crystals in the fiber.

The sharp drop in crystallinity shown in Figure 3 would be expected to reduce the modulus of the sample. The mechanical spectra in Figure 2 show that the drop is greatest at low temperature, well below the  $T_g$  of the original samples. Chemical changes in the amorphous material or suppression of the glass transition should have little effect at low temperatures. At temperatures above the original glass transition, the storage modulus is initially reduced by formalization, and then increases again. Here crosslinking of the amorphous material should significantly stiffen the sample. Qualitatively it seems clear that the loss in crystallinity is again responsible for the loss in modulus, and then continuing crosslinking counterbalances this effect.

The general trend for crystal size as determined by wide angle X-ray diffraction is that the crystals become significantly shorter in the chain direction and do not change their width. It would be desirable to relate these structural changes as well as the crystallinity loss to the mechanical properties observed, but this is difficult. A mechanical model for the fiber is required, and any model acceptable for high modulus fibers has many parameters that might be changed by chemical treatment. In a Takayanagi type series-parallel model where the block representing the fibrous crystals is mechanically in series with a small amount of softer disordered material,<sup>20,21</sup> the model parameters need have no direct relation to the observed crystal size. In this model, the microfibrils are the stiff load bearing element, and the important parameters are the fraction of the sample cross section that is taken up by the fibrous crystals,  $b$ , and a measure of the stiffness of the fibrils. In the discontinuous crystal model, this stiffness is controlled by the fractional amount of disordered material in series with the fibrous crystals,  $f$ , and the modulus of this disordered material.  $(1 - f)$  is the fractional length of the fibrous crystal block.

It is natural to associate a reduction of crystal length along the chain direction with a drop in  $(1 - f)$  and a change in crystal width with a change in  $b$ . Complete destruction of crystals would also reduce  $b$  while the mean crystal size of the remaining crystals might increase or decrease. The fact that crystallinity falls by 1/3, while the mean crystal volume falls only 20% indicates that crystals are indeed being completely destroyed.

By assuming that the amount of fibrous crystal in the model,  $b(1 - f)$ , is reduced proportionally with the fall in total crystallinity and that the modulus of the disordered material at very low temperatures is unaffected by formaldehyde treatment, it is possible to calculate the model parameters in various cases. It was found that reasonable values were obtained if it was assumed that the chemical treatment affected only  $f$ , or affected  $b$  and  $f$  equally. Assuming that  $f$  remained constant and that only  $b$  was affected did not give reasonable values. The mechanical modeling can give no quantitative results, but it shows that the mechanical and structural data are consistent with the chemical attack of crystal end surfaces. Under the conditions of the

chemical treatment, in water at 72°C, very small crystals of PVAI will become unstable and dissolve. It is possible that crosslinking PVAI fibers at lower temperatures, perhaps by radiation, using  $\gamma$  radiation or high-energy electrons, may be more successful in improving mechanical properties. Crosslinking at lower temperatures and not in the presence of solvents should help preserve the crystals.

### CONCLUSIONS

Treatment of highly drawn PVAI fibers with formaldehyde solution at 72°C does crosslink the amorphous material rapidly and uniformly. This suppresses  $T_g$  and so reduces the drop in modulus on heating the fiber. However, the treatment also reduces crystallinity by 1/3 and the net effect is to reduce the fiber modulus at room temperature to about half its original value. The drop in modulus is worse for the higher modulus fibers. X-ray diffraction shows the crystals in the fiber to be quite small originally, and on average they are reduced in length, along the fiber direction, and not in width by the chemical treatment.

This work was financially supported by the National Science Foundation. Also, we wish to express our thanks to Dr. Wade Adams of Wright-Patterson AFB for the loan of the Braun position sensitive X-ray detector and for assistance with experiments at CHESS.

### References

1. I. Sakurada, *Polyvinyl Alcohol Fibers*, Dekker, New York, 1985.
2. H. Kwon, S. Kavesh, and D. Prevorsek, U.S. Pat. 4 440 711 (1984).
3. H. Tanaka, S. Suzuki, and F. Ueda, Eur. Pat. Appl. 146,084 (1984).
4. P. Lemstra, C. Bastiaansen, and H. Meijer, *Angew. Makromol. Chem.*, **145** / **146**, 343–358 (1986).
5. M. Amano and K. Nakagawa, *Polym. Commun.*, **28**, 119–120 (1987).
6. P. Cebe and D. T. Grubb, *J. Mater. Sci.*, **20**, 4465–4478 (1985).
7. P. D. Garrett and D. T. Grubb, in *Morphology of Polymers*, B. Sedlacek, Ed., de Gruyter, Berlin, 1986.
8. P. D. Garrett and D. T. Grubb, *J. Mater. Res.*, **1**(6), 861–869 (1987).
9. P. Garrett and D. Grubb, *Polym. Commun.*, **29**, 60–63 (1988).
10. I. Sakurada and H. Nakamura, *Kobunshi Kagaku*, **8**, 430 (1980) (from Ref. 1, p. 218).
11. K. Kawase, O. Morimoto, and T. Mochizuki, Japanese Chem. Soc. Annual Meeting Reports (1968), reported in *Polyvinyl Alcohol, Properties and Applications*, C. A. Finch, Ed., Wiley, London, 1973, pp. 397–402.
12. I. Sakurada and K. Fuchino, *Riken Iho*, **20**, 898 (1941).
13. I. Sakurada and O. Yoshizaki, *Kobunshi Kagaku*, **10**, 315 (1953).
14. J. G. Pritchard, *Poly(Vinyl Alcohol): Basic Properties and Uses*, Gordon and Breach, London, 1970.
15. D. T. Grubb, *J. Mater. Sci. Lett.*, **3**, 499–502 (1984).
16. Monsanto Technical Bulletin No. 6070D (undated).
17. J. Sauer and A. Woodward, in *Thermal Characterization Techniques*, P. Slade and L. Jenkins, Eds., Dekker, New York, 1970.
18. R. Tubbs and T. K. Wu, in *Polyvinyl Alcohol, Properties and Applications*, C. A. Finch, Ed., Wiley, London, 1973.
19. L. Mandelkern, D. Roberts, A. Diorio, and A. Posner, *J. Am. Chem. Soc.*, **81**, 4148 (1959).
20. M. Takayanagi, K. Imada, and T. Kajiyama, *J. Polym. Sci. C*, **15**, 263 (1966).
21. D. T. Grubb, *J. Polym. Sci. Polym. Phys. Ed.*, **21**, 165 (1983).

Received August 16, 1988

Accepted January 17, 1989